Planta (2007) 225:451–468
DOI 10.1007/s00425-006-0359-0

ORIGINAL ARTICLE

Actin is bundled in activation-tagged tobacco mutants that tolerate aluminum

Abdul Ahad · Peter Nick

Received: 12 March 2006 / Accepted: 10 July 2006 / Published online: 15 August 2006

Abstract A panel of aluminum-tolerant (*AlRes*) mutants was isolated by protoplast-based T-DNA activation tagging in the tobacco cultivar SR1. The mutants fell into two phenotypic classes: a minority of the mutants were fertile and developed similarly to the wild type (type I), the majority was male-sterile and grew as semi-dwarfs (type II). These traits, along with the aluminum tolerance, were inherited in a monogenic dominant manner. Both types of mutants were characterized by excessive bundling of actin microfilaments and by a strongly increased abundance of actin, a phenotype that could be partially phenocopied in the wild type by treatment with aluminum chloride. The actin bundles could be dissociated into finer strands by addition of exogenous auxin in both types of mutants. However, actin microfilaments and leaf expansion were sensitive to blockers of actin assembly in the wild type and in the mutants of type I, whereas they were more tolerant in the mutants of type II. The mutants of type II displayed a hypertrophic development of vasculature, manifest in form of supernumerary leaf veins and extended xylem layers in stems and petioles. Whereas mutants of type I were characterized by a normal, but aluminum-tolerant polar auxin-transport, auxin-transport was strongly promoted in the mutants of type II. The phenotype of these mutants is discussed in terms of reduced endocytosis leading, concomitantly with aluminum tolerance, to changes in polar auxin transport.

Keywords Actin microfilaments · Activation tagging · Aluminum tolerance · Auxin transport male sterility tobacco (*Nicotiana tabacum* L.)

Abbreviations

Al	Aluminum
AlRes	Aluminum tolerance
MS	Murashige and Skoog medium

Introduction

Aluminum (Al), among the most abundant metals in soils, is usually inactivated by complexation. However, free Al ions are released at low pH, often in consequence of pollution or intense agricultural activity. Globally, more than a third of cultivated land is estimated to suffer from Al toxicity in consequence of soil acidification. The problem is particularly serious in the tropics and subtropics. The toxicity of Al thus poses severe constraints to plant growth and agricultural productivity worldwide (Foey et al. 1978) with root growth being a major (for review see Delhaize and Ryan 1995) and very early target (Blancaflor et al. 1998).

The cellular response to Al is complex and the molecular mechanisms of Al toxicity are still far from being understood. Investigations on Al uptake have demonstrated that Al affects the properties of the plasma membrane (Wagatsuma et al. 1995) after binding to pectic components of the cell wall (Chang et al. 1993). Thus, Al does not necessarily need to enter the

A. Ahad (✉)
Umeå Plant Science Centre, Department of Plant Physiology, Umeå University, 90187 Umeå, Sweden
e-mail: abdul.ahad@plantphys.umu.se

P. Nick
Botanisches Institut 1, University of Karlsruhe, Kaiserstr. 2, 76128 Karlsruhe, Germany

target cell to become effective (for review see Sivaguru et al. 2000). Intracellular responses to Al involve rapid changes in the organization of the Golgi apparatus accompanied by reduced secretion (Bennet and Breen 1991), and rapid changes of the cytoskeleton that occur concomitantly with Al-induced changes of root growth. Bundles of cortical microtubules increase in number during the first hour of exposure (Schwarzerová et al. 2002), which upon prolonged incubation is followed by reorganization and/or bundling of microtubules depending on time of exposure and physiological state of the tissue (Blancaflor et al. 1998). Actin microfilaments respond by increased bundling accompanied by increases of mechanical rigor (Grabski and Schindler 1995).

These cytoskeletal responses could be triggered indirectly through the cell-wall cytoskeletal continuum in consequence of the primary Al response in the apoplast. On the other hand, even minute concentrations of active Al in the cytoplasm might be sufficient to affect the cytoskeleton by inhibiting GTPase or ATPase functions of tubulin and actin—it was shown for tubulin assembly that Al binds the GTP-binding site of tubulin with extremely high affinity (MacDonald and Martin 1988) and this has been invoked to explain Al-induced toxicity in neural cells (Schmidt et al. 1991). Alternatively, Al might affect the cytoskeleton through interference with vesicle traffic, since a treatment of tobacco cells with Brefeldin A was shown to increase the Al tolerance (Vitorello and Haug 1999).

Recent evidence, however, suggests that Al interferes with signalling chains that interfere with the cytoskeleton: in roots of thale cress, there is evidence for a glutamate receptor that regulates cortical microtubules and is activated upon treatment with Al (Sivaguru et al. 2003a, b). In the roots of maize auxin transport has been identified as a major target of Al toxicity—application of $AlCl_3$ to the root inhibited polar transport of radioactively labelled auxin (Kollmeier et al. 2000), and shifted the regional patterning within the root tip in a way similar to inhibitors of polar auxin transport (Doncheva et al. 2005)

Plants have obviously evolved strategies to cope with increased Al incidence, since accumulation of Al in the foliage is widely found especially among ancient families of dicotyledonous plants inhabiting tropical rain forests (Chenery and Sporne 1976). Secretion of Al chelators such as malate, oxalate or citrate into the rhizophere has been proposed as the most effective tolerance mechanism to neutralize Al prior to contact (Ryan et al. 1995; Yang et al. 2005). This is supported by first biotechnological approaches, where overexpression of a bacterial citrate synthase (CS) gene in transgenic tobacco and papaya plants was reported to confer Al tolerance (de la Fuente et al. 1997), although later attempts to reproduce these results failed (Delhaize et al. 2001). In wheat, Al was recently shown to induce expression of a malate transporter. Since malate forms a stable complex with Al that seems to be harmless for plants, this could provide a mechanism for Al tolerance to wheat (Sasaki et al. 2004). Extensive comparative physiological studies in maize roots, however, indicated that in addition to organic acids released form the root there exist additional mechanisms for Al resistance and sensitive species (Piñeros et al. 2004; also see review Kochian et al. 2005). To identify the tolerance mechanisms alternative attempts were taken that include search for genes that are upregulated in response to Al and indicate a strong role for signalling events and oxidative burst (Watt 2003).

If signalling has an impact on the Al response of a plant, it should be possible to generate dominant mutations by a gain-of-function approach, where signalling events that culminate in Al tolerance are upregulated (Chang et al. 1993). This can be achieved through activation tagging (Hayashi et al. 1992; Koncz et al. 1994), where multiple transcriptional enhancer elements will *cis*-activate genes adjacent to the integrated tag creating a dominant trait that could be selected already in primary transformants. In fact, activation tagging has been a successful approach in the search for components of hormonal, developmental or pathogen responses (cytokinins: Kakimoto 1996; Zubko et al. 2002; plant architecture: Nakazawa et al. 2003; pathogen resistance: Weigel et al. 2000; Xia et al. 2004) and is increasingly used as a tool for functional genomics (for a recent review see Tani et al. 2004).

In a previous publication (Ahad et al. 2003), we have used activation tagging to isolate tobacco mutants with reduced microtubular turnover and could demonstrate that these mutants are endowed with increased tolerance to cold stress. In the present work, we transfer this approach to the study of Al tolerance. We report on two groups of mutants that are Al tolerant. Two mutant lines are fertile and of normal growth habit. However, the majority of mutant lines falls into a second group: they are male sterile semi-dwarfs. This peculiar correlation of Al resistance and reduced growth should allow insights into the cellular responses to Al. We therefore focussed on both group of mutants in relation to their bundled actin microfilaments and what can be phenocopied in the wild type by treatment with Al. This actin phenotype in the mutant can be rescued by exogenous auxin. We further observe increases of polar auxin fluxes accompanied by hypertrophic vasculature in leaves and stems. We interpret

the phenotype of these mutants in the context of changed vesicle traffic that causes, in parallel to Al tolerance, changes in polar auxin transport.

Materials and methods

Isolation and propagation of Al-tolerant mutants

SR1 (*Nicotiana tabacum*, cv. Petit Havana) tobacco plants (kindly gifted by Gunther Neuhaus Laboratory, University of Freiburg, Germany) that had been raised under sterile conditions were used for the isolation of protoplasts as described (Ahad et al. 2003). Protoplasts were transformed after 1 week in liquid culture when most of the cells passed through their second division. After 48 h of co-cultivation with freshly grown bacteria (*Agrobacterium tumefaciens*, strain GV3101), micro-calli were cultivated in the presence of 15 mg/l hygromycin and 200 μM $AlCl_3$ (Sigma). Preliminary dose-response studies with untransformed protoplasts had shown that selection with 200 μM $AlCl_3$ was stringent enough to suppress any growth activity (reference to free Al values obtained by GeoChem). To determine plating efficiency, an aliquot of cells was cultured in the absence of hygromycin. All plates contained 150 mg/l of cefotaxim and 75 mg/l ticarcillin (both Duchefa) to suppress bacterial growth. Within 3 weeks, very minute but vigorously dividing calli were transferred onto solid MS plates for regeneration maintaining the selective pressure (hygromycin, $AlCl_3$). After rooting, plantlets were transferred to the green house for seed set. In case of male-sterile lines of type II, flowering plants were pollinated with pollen from untransformed SR1 wild type. To test the stability of the trait, seeds of the mutants were sown on solid MS medium (0.8% w/v agar) complemented with 200 μM $AlCl_3$ and 15 mg/l hygromycin and raised in the dark at 25°C and digital images of the plates recorded (Coolpix, Nikon, Tokyo, Japan) 2 weeks after sowing. Leaf areas were measured from those images by the Scion Image software (Scion Corporation, Frederick, MD, USA) using at least 100 individuals per assay.

Strains and vectors

The *Agrobacterium* strain GV 3101 was transformed with the pPCV Tac 7 activation-vector as described previously (Koncz et al. 1990). This vector contains a tetrameric enhancer sequence at the left border and a hygromycin resistance gene as plant-selectable marker at the right border in addition to the bacterial origin of replication and ampicillin/carbenecillin genes for selection in *E.coli* or *Agrobacterium*, respectively. Details of bacterial cultivation and transformation are described (Ahad et al. 2003).

Fertility assays

At least four mutant lines were unable to set seed. By symmetrical crosses with the SR1-wild type it could be shown that these mutants were male sterile. To check the pollen phenotype, fresh pollen from SR1 and different mutants were incubated on microscopic slides with 1 mM DAPI overnight in a humid chamber at 4°C. Next morning, they were viewed by epifluorescence microscopy (Axioskop, Zeiss, Giessen, Germany) using a conventional DAPI filter set. These male-sterile lines were maintained by pollination with pollen from untransformed SR1 donors that had been raised simultaneously.

Estimation of cell length

Epidermal peels were obtained from internodes of plants that had been raised in parallel for 3 weeks in the greenhouse. Internodal peels from wild type and mutants were mounted in water and digital bright-field images recorded (Axiovision, Zeiss). The lengths of epidermal hairs and trichome cells were determined from those images in at least two independent experimental series comprising at least five peels from different individuals.

Root-growth assay

Seedlings of wild type (SR1) and the mutant lines *AlRes4* and *AlRes5* were raised on 0.8% (w/v) of water-agar dissolved in water or different solutions of $AlCl_3$ rather than in MS medium. In order to measure root length, the plates were sealed and kept vertically, such that the roots could grow parallel to the agar surface. Root growth was recorded by a digital camera in relation to a size standard and elongation rates determined over a period of 4 weeks. Since the addition of $AlCl_3$ leads to acidification of the medium (Table 3), parallel control was done, where different pH values were adjusted with and without $AlCl_3$ by buffering with 25 mM Mes.

Visualization of actin filaments

Actin microfilaments were stained in the petioles of plants that had been raised for 2 weeks in the greenhouse following a modified version of the protocol described previously (Waller and Nick 1997). Petioles

were incubated at 25°C on a shaker for 2 h with water containing 0, 50, 100 and 200 μM concentrations of $AlCl_3$. *Notabene*: here Al was not administered through the roots, but directly to petioles as target tissue. In the experiment shown in Fig. 4, the petioles were incubated for the same time in the absence of $AlCl_3$ with 10 nM of the actin inhibitor latrunculin B (Sigma) with 10 μM of indolyl-3-acetic acid (+ auxin) or in the absence of added auxin. The tissue was fixed for 15 min in 1.8% (w/v) paraformaldehyde dissolved freshly in 100 mM potassium-phosphate buffer complemented with 100 mM KCl. Directly after washing, epidermal peels were obtained from the fixed material and incubated in the dark with a drop of 240 nM FITC-phalloidin at 37°C for 1 h. After washing three times, the samples were immediately viewed either under an epifluorescence microscope using a narrow-band GFP filter-set (filter-set 15, Zeiss) or under a confocal laser scanning microscope (DM RBE; Leitz, Bensheim, Germany) with excitation at 488 nm by an argon-krypton laser, a beam splitter at 510 nm, and a 515-nm emission filter.

SDS-PAGE and Western analysis

Leaves from plants raised in the greenhouse were excised, cut into sections of equal size (4 × 4 mm) and incubated for 2 h with different concentrations of $AlCl_3$ (i.e. 0, 50, 100 and 200 μM). Again, $AlCl_3$ was here administered directly to the target tissue, not via the roots. After washing three times with de-ionized water, the leaf pieces were shock-frozen in liquid nitrogen and ground in a mortar with liquid nitrogen until a very fine powder was obtained. Total proteins were extracted as described previously (Nick et al. 1995). Protein concentrations were determined from 10-μl aliquots by the amido-black protocol (Popov et al. 1975). Soluble fractions and total membrane fractions were extracted according to Waller et al. (2002). The proteins were analysed by conventional sodium-dodecyl sulphate polyacrylamide-gel electrophoresis (SDS-PAGE) and Western blotting, as described in Nick et al. (2000), loading 6 -10 μg of total protein per lane. α-tubulin was probed with the monoclonal rat antibody YOL 1/34 (Abcam, London, UK) that is targeted to a conserved epitope (residues 414–422) present in all eukaryotic α-tubulins (Breitling and Little 1986). Actin was probed with the mouse monoclonal antibody pan-Ab5 (Dunn Labortechnik, Mainz, Germany) and used in a dilution of 1:150. The secondary antibody directed against rat or mouse IgG, respectively, were conjugated to horseradish peroxidase and used in a dilution of 1:2,000 (Sigma). The signals were visualized by bioluminescence (ECL; Amersham-Pharmacia) and recorded on X-ray films. Protein abundance was quantified using the integrated density algorithm of the Scion Image Software (Scion Corporation) using the total integrated density of the blot as internal reference.

Isolation of nuclei from leaf tissues

Nuclei were isolated from leaf tissues of wild type and mutants with a modified version of the protocol described previously (Koop et al. 1996): leaves were cut into small pieces and incubated on water, with or without $AlCl_3$, for 2 h (i.e. Al was administered not through the roots, but directly to the target tissue). The leaf tissue was then washed thoroughly with water and ground with quartz sand on ice in a mortar, with 12 ml of nuclei-isolation buffer (10 mM Mes pH 5.5, 10 mM NaCl , 10 mM KCl, 2.5 mM EDTA, 2.5 mM 2-mercapthoethanol, 0.1 mM spermidine, 250 mM manitol and 0.6% v/v Triton X-100) per gram fresh weight. The resulting suspension was passed through a 50-μM nylon filter into a 50 ml falcon tube and then transferred onto a discontinuous Percoll (Amersham) gradient consisting of 4 ml of 67% v/v Percoll and 2 ml of 43% v/v Percoll in nuclei-isolation buffer. The loaded tube was then spun down for 5 min at 1,000*g*. Nuclei were collected from the 43%/67% interphase and washed by dilution with 10 ml nuclei-isolation buffer and centrifugation for 5 min at 600*g*. The sediment that was enriched in the nuclei was analysed by SDS-PAGE and Western blotting as described above.

Leaf-disc assay for cell expansion

Leaves of comparable size from plants that had been raised under sterile conditions were subdivided into squared pieces of 5 mm length and placed onto solid MS medium (0.8% w/v agar) supplemented with different concentrations (i.e. 0, 0.1, 1, and 10 nM) of the actin inhibitor latrunculin B (Sigma) supplemented with 0.03 mg/l naphthyl-acetic acid (NAA) and 1 mg/l kinetin to support cell growth. The plates were cultured in a phytotron with a cycle of 16 h light and 8 h dark. Digital images of the plates were recorded (Coolpix, Nikon) 2 months after the onset of the experiment. Leaf areas were measured from those images by the Scion Image software (Scion Corporation) using at least 20 individuals per experiment.

Leaf veins and stem vasculature

Leaf veins images were recorded from mutant and wild-type plants that had been grown for 2 weeks in

the greenhouse by a digital camera (Cooplix 990, Nikon). To observe stem anatomy, hand-made cross sections of petioles and internodes were incubated with phloroglucinoethyl (Serva) and a few drops of HCl for 15 min. The sections were washed three times with distilled water and viewed by brightfield microscopy (Axioskop); images were recorded digitally (Axiovision).

Auxin-transport assay

For the auxin-transport assay, petioles from plants that had been raised for 3 weeks in the greenhouse were used. Petiole segments of 6 mm length were excised, marked by incisions on apical and basal ends, and incubated for 1 h in liquid MS medium (Murashige and Skoog 1962) on a topover-shaker. The medium also contained 0.1 μM IAA supplemented with or without 200 μM $AlCl_3$. Again, Al could here access the target tissue directly, not through the roots. The pre-treated segments were placed in a humid chamber between two agar blocks (4 × 4 × 1 mm, 1.5% agar) on a glass-slide carrier. The donor agar-block containing approximately 10,000 cpm of ^{3}H-IAA (American Radiolabeled Chemicals, St. Louis, MO, USA) was placed into contact with the apical end of the segments (Godbolé et al. 2000), whereas the receiver block (void of ^{3}H-IAA) was brought into contact with the bottom end of the segments. After incubation for 2 h at 25°C in a moist chamber, the set-up was carefully disassembled and donor blocks, receiver blocks, and petiole segments collected separately in scintillation vials filled with 500 μl of 10 mM Tris. In some experiments, the petiole segments were subdivided into four sections after auxin transport and were collected separately. Each vial was filled with 5 ml of scintillation fluid (Rotiszint, Roth, Karlsruhe, Germany) and incubated in the dark at 25°C for 2 h on an orbital shaker. Radioactivity was determined as cpm by means of a fluid-scintillation counter (LS 5000CE, Beckman). The counting error was negligible since each sample was counted twice 15 min each (data not shown). Each data set was reproduced at least triplicate at different days using five to ten segments from different individuals per experiment.

Results

The recovered mutants are tolerant to Al

Only a small number of mutants were selected from a large number of protoplasts (Table 1). This might reflect the specificity of the screen, but, alternatively, could be caused by a high number of false positives that had survived the cocultivation with Agrobacterium, although they did not harbour the plasmid. To discriminate between these possibilities, equal aliquots of the cocultivated protoplasts were either plated on medium without (−hygro) or with hygromycin (+ hygro), and the number of surviving cells was quantified after growth for further 3 weeks. The resulting numbers were identical (Table 1) speaking against a significant fraction of false positives. Thus, the vast majority of cells that had survived the cocultivation, apparently carried the hygromycin resistance marker and therefore presumably the activation tagging vector as well. This suggests that it was the stringency of the screen that was responsible for the low number of putative mutants. In our hands, not a single protoplast of non-transformed controls survived even under screening conditions that were less stringent as those employed to select the mutants (data not shown).

The surviving protoplasts were regenerated into plants that were self-pollinated (defined as original generation T_0). The seeds of those primary transformants (generation T_1) were again subjected to selection by $AlCl_3$ and/or hygromycin. For a smaller group of mutant lines ("type I"), non-segregating populations that exhibited tolerance to Al along with hygromycin resistance could be obtained already from generation T_2 and have remained stable through two to three subsequent generations obtained so far. For a larger group of mutant lines ("type II"), we observed male sterility (see below) and we had to maintain these lines by cross-fertilization with wild-type pollen. The offspring

Table 1 Transformation efficiency and stringency of the screen

Input	Transformation control		No. of cells on $AlCl_3$ selection	Recovered colonies	Putative mutants	
	-hygro	+hygro			Type I	Type II
29.4×10^6	3×10^6	3×10^6	23.4×10^6	48,707	2	5

The initial number of protoplasts used for the experiment is indicated under 'input'. After cocultivation, aliquots were grown with or without hygromycin to estimate the number of transformed cells. The number of colonies recovered immediately after the screen is indicated as well as the number of putative mutant plants that could be obtained from those colonies under continuation of the selective pressure

Table 2 Segregation of the offspring from F1 plants produced by back-crossing wild-type (SR1) pollen donor to mutant pollen acceptors for the mutant lines *AlRes4* and *AlRes5* under combined selection pressure with hygromycin (15 mg ml^{-1}) and $AlCl_3$ (200 μM) for a period of 4 weeks

Mutants	Resistant (R)	Sensitive (S)	Observed ratio R/S	Expected ratio for one insertion
AlRes4	226	59	79%/21%	75%/25%
AlRes5	171	157	52%/58%	58%/42%

Resistant plantlets were green, and displayed expanded cotyledons and well-developed leaflets, sensitive plantlets were chlorotic or even bleached, dwarfed, cotyledons were closed, and leaflets not developed. For *AlRes4*, a putatively homozygous line was used, such that all F1-plants were expected to be heterozygotes. For *AlRes5*, the F1 plants displaying the resistant phenotype could either carry one or two of the dominant mutant alleles, with expected frequencies of 2/3 with one and 1/3 with two alleles

of these lines was segregating into Al-sensitive and Al-tolerant individuals, similar segregations were observed, when the offspring was plated on hygromycin, and in the tolerant individuals a Southern probe specific for the T-DNA insertion labelled a band not observed in the sensitive individuals (data not shown). This pattern has remained stable through the two to three subsequent generations obtained so far. For some of the lines we tested segregation of resistance to combined selection with hygromycin and $AlCl_3$-resistance in the offspring of F1-plants resulting from back-crosses between wild-type (SR1) pollen donor and mutant pollen acceptors (Table 2). The observed segregation rates were consistent with a model with one T-DNA insertion.

Owing to the male sterility it was difficult to test mutual complementation of the different mutants of "type II". We therefore focussed our subsequent analysis on two mutants—*AlRes4* as representative of the fertile "type I" group of mutants, and *AlRes5* as representative of the male sterile "type II" group. Figure 1 shows the response of seedlings that had been raised on medium without Al as compared to medium containing 200 μM $AlCl_3$. Cotyledons of WT seedlings are significantly ($P = 0.01$) reduced by about 50% in area, when Al was present (Fig. 1a, b). For *AlRes4*, cotyledons are smaller as compared to the WT, but they increase in area upon treatment with Al, i.e. the sign of the response is reverted. However, this difference is statistically not significant ($P = 0.1$). For *AlRes5*, the area is more or less similar to the wild type as long as Al is absent. In the presence of Al, the population segregates into individuals with small cotyledons and those with large cotyledons (Fig. 1a, b); this segregation is even more pronounced, when the offspring of Al-selected F1-plants is analysed (Fig. 1c). One subpopulation behaves similar to the wild type, i.e. leaf size is reduced in response to Al; the other subpopulation responds by increased leaf size.

Since the primary target of Al is the root, we tested the response of root growth to $AlCl_3$ (Fig. 1d, e). After an initial phase of strong elongation roots were observed to reach steady-state growth from 2 weeks after germination (Fig. 1d) with a comparable rates between 0.5 and 0.6 cm $week^{-1}$ for WT, *AlRes4* and *AlRes5*. When steady-state growth rates are plotted over the concentration of $AlCl_3$ in the medium (Fig. 1e), roots of the WT are observed to become inhibited down to 0.1 cm $week^{-1}$ for 200 μM $AlCl_3$ corresponding to 15% of the water control. For *AlRes4*, at 200 μM $AlCl_3$ the growth rate is still at 0.2 cm $week^{-1}$ (corresponding to 40% of the water control), and for *AlRes5*, even a growth rate of 0.3–0.4 cm $week^{-1}$ is maintained (corresponding to more than 50% of the water control). This shows that root growth in the mutant is more persistent to treatment with $AlCl_3$. This difference is already significant ($P = 0.01$) for *AlRes5* from 50 μM of $AlCl_3$ and for *AlRes4* from 100 μM of $AlCl_3$.

Since $AlCl_3$ results in acidification of the medium (Table 3), we tested whether acidification per se would impair growth. For this purpose, we adjusted, in the absence of $AlCl_3$, the pH to a value normally reached by 100 μM $AlCl_3$, but we could not observe any change in growth as compared to roots growing in water (data not shown). Conversely, when 200 μM $AlCl_3$ were administered keeping the pH constant, root growth was observed to become inhibited in the wild type, but even increased in the mutants (data not shown). We conclude that $AlCl_3$-dependent acidification cannot account neither for the inhibition of root growth in response to $AlCl_3$ nor for the differences between wild type and mutants.

Adult plants of *AlRes4* were indistinguishable from the wild type with respect to height, internode length (Fig. 2a) and fertility (Fig. 2e). The same was true for the other member of the "type I" group, *AlRes7*. In contrast, *AlRes5* (along with the majority of the other mutants of "type II") showed a reduction in height by about 40%, due to a drastic reduction of internode length by about 80% (Fig. 2a, b). Interestingly, the number of nodes at the onset of flowering was almost doubled as compared to the WT accompanied by the formation of nodal flowers (Fig. 2d). All mutant lines (for both "type I" and "type II" mutants) were of "hairy" appearance. This was due to increased length of trichome cells at maintained or

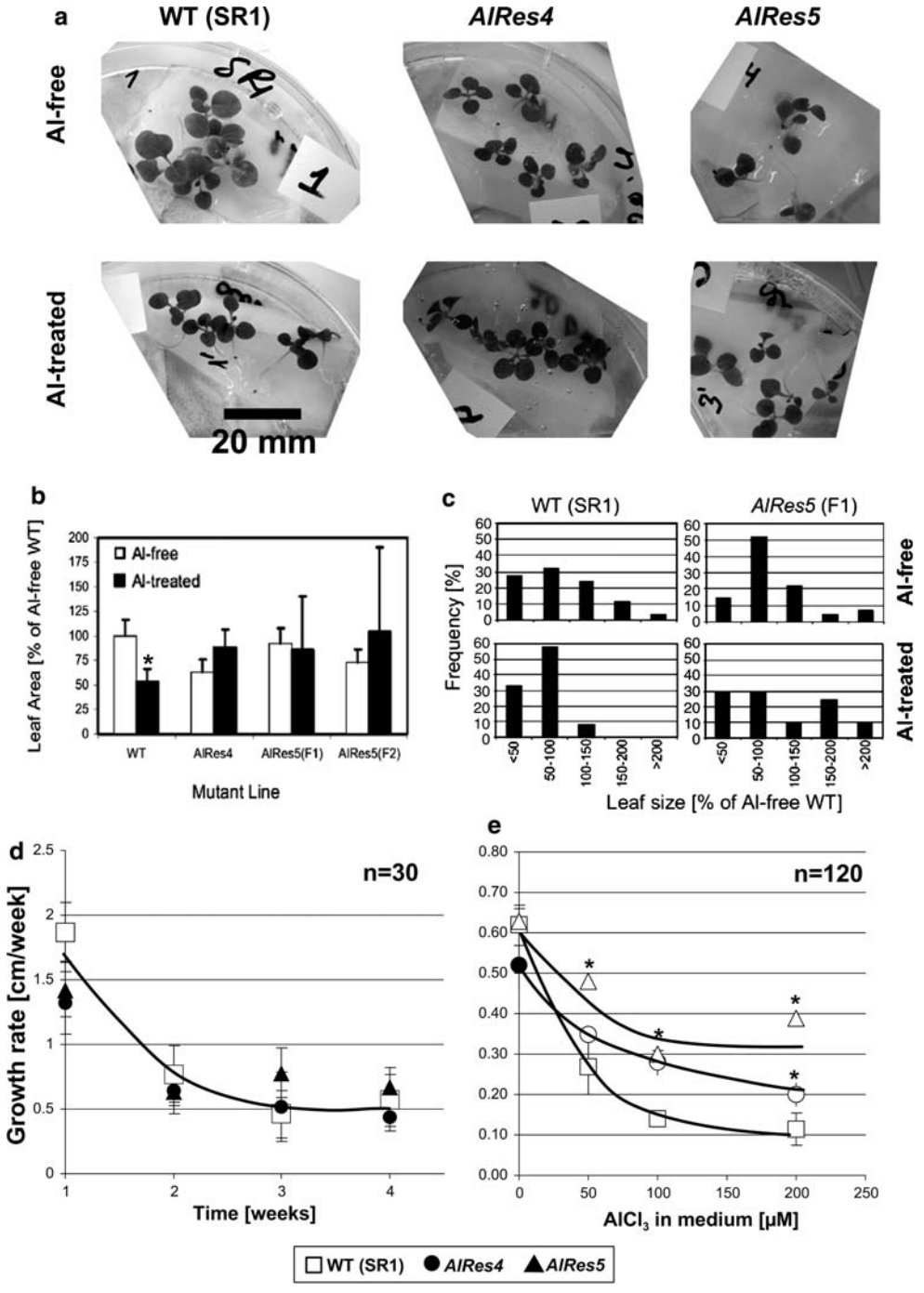

Fig. 1 **a–e** Activation-tagged *AlRes* mutants are Al tolerant. **a** Phenotype of young seedlings that had been raised in the absence of hygromycin for 3 weeks on Al-free medium or on medium that was supplemented with 200 µM of $AlCl_3$. Representative images are shown for the wild type (SR1), for the homozygous line *AlRes4*, and for the line *AlRes5* that had to be maintained as heterozygous line in consequence of male sterility. **b** Leaf area of seedlings treated as described in **a** for the wild type (SR1), *AlRes4*, and for two generations of *AlRes5*. One hundred individuals were scored for each data point. The error bars indicate standard deviations. The *asterisk* indicates a difference between the untreated control and the sample treated with $AlCl_3$ statistically significant with $P = 0.01$ (t test). Note the large standard deviation for $AlCl_3$-treated *AlRes5* and the absence of a statistically significant difference in the mutants. **c** Frequency distribution over leaf area for seedlings of WT (SR1) and heterozygous *AlRes5*. Note segregation of Al-treated *AlRes5* into subpopulations with large and small leaf area, respectively. The *abscissa* indicates leaf area in relative units—100% correspond to the average area of the wild type. **d** Changes of root growth in seedlings of the wild type (SR1), *AlRes4*, and *AlRes5* raised on Al-free medium. Growth rate is plotted over the time after germination. **e** Dose-response of steady-state growth over the concentration of $AlCl_3$ in the medium for wild type (SR1), *AlRes4*, and *AlRes5*. *Asterisks* indicate values, where the mutants are significantly different from the respective wild-type value ($P = 0.01$)

even slightly increased cell numbers as exemplarily shown for *AlRes 5* (Fig. 2c). Nuclei could be visualized by DAPI in the pollen of WT or mutants of "type I", but not in pollen from mutants of "type II", such as *AlRes5* (Fig. 2e), consistent with the complete failure to obtain seeds after self-pollination in these mutant lines. However, viable seed could be obtained after cross-pollination with pollen from WT plants.

These characteristic traits (Al tolerance, Hyg-resistance, hairiness for "type I"mutants; in addition reduced internode length and male sterility for "type II" mutants) by now have been stable and linked over several generations. It should be noted that the morphological and developmental changes of "type II" mutants did not require the presence of Al to be manifest and were also observed, when the plants had never been challenged with $AlCl_3$.

Actin microfilaments are bundled in Al-tolerant mutants

Mutants of type I are of basically normal appearance, but are tolerant to $AlCl_3$, which is also true for root growth. The phenotype of type I mutants would be consistent with a mechanism, by which Al^{3+} ions are prevented from entering the roots, for instance by excretion of chelating organic acids (Ryan et al. 1995; Yang et al. 2005). It is more difficult to interpret the phenotype of type II mutants in the same way since they show, in addition to their Al-tolerance, a strong phenotype in the absence of Al-challenge (stunted growth, male sterility). The analysis of those mutants might therefore allow insights into cellular targets related to the Al response. We therefore focussed our analysis to the physiological and cell biological base of the type II phenotype.

As a first attempt to get insight into the stunted habitus of "type II" mutants, we analysed the organization of the cytoskeleton in epidermal cells. Preliminary experiments had shown that the orientation of cortical microtubules was diverted towards more longitudinal arrays (data not shown). However, since arrays of different orientation coexisted in a given population, the differences between the lines were relatively marginal. We therefore focussed on actin microfilaments.

In epidermal cells of untreated wild type, actin microfilaments were arranged in fine strands parallel with the long axis of the cell (Fig. 3a). Near the cell poles, a fine mesh of cortical filaments became visible upon confocal microscopy (Fig. 3b). In response to treatment with $AlCl_3$ we observed supernumerary actin microfilaments emerging from the nuclear envelope (Fig. 3c) that with increasing concentrations merged into thicker bundles of actin (Fig. 3d).

In both mutants, *AlRes4* (Fig. 3e) and *AlRes5* (Fig. 3h), a characteristic array of radial microfilament bundles, emanated from the nuclear envelope even without Al treatment. This conspicuous difference did not change much, when Al was added except a slight tendency for more bundled microfilaments as compared to the untreated samples (Fig. 3f, g, i, j).

Thus, the situation in the mutants (radial arrays of numerous microfilament bundles emanating from the nucleus) can be mimicked in the wild type by treatment with Al. In other words, actin microfilaments in the mutants behave in the absence of Al similar to a wild type treated with Al. It is noteworthy that not only *AlRes4* and *AlRes5*, but all mutants showed this phenotype (data not shown), irrespective of their classification into "type I" or "type II".

In the next step we asked, whether auxin, known to dissociate microfilament bundles into finer strands (Holweg et al. 2004) and to relax actin tension (Grabski and Schindler 1995), would rescue the mutant phenotype in terms of actin organization. In the wild type, the addition of auxin did not cause significant changes in the structure or number of actin microfilaments (Fig. 4a), which is possibly related to the fact that microfilaments were already mostly arranged in fine strands prior to the treatment with auxin. In contrast, the bundled microfilaments typically found in untreated mutant cells were at least partially replaced by finer strands of actin bringing the mutant closer to the wild type situation (Fig. 4a). Thus, the mutant phenotype (bundled actin even in the absence of Al) can be (partially) rescued by the addition of exogenous auxin.

As to detect potential changes in actin turnover between wild type and mutant, we assessed the response to latrunculin B, a drug that prevents addition of G-actin to the growing ends of microfilaments. The sensitivity of microfilaments to latrunculin B is expected to depend on the rate of treadmilling with dynamic microfilaments being more sensitive as compared to microfilaments with a low rate of monomer exchange. We observed that actin microfilaments were completely destroyed by latrunculin B in WT and *AlRes4*, whereas the microfilament bundles in *AlRes5* were more recalcitrant and persisted despite considerable changes in orientation (Fig. 4a, right-hand lane).

Since it is difficult, if not impossible, to quantify these differences in actin persistence on a cellular level,

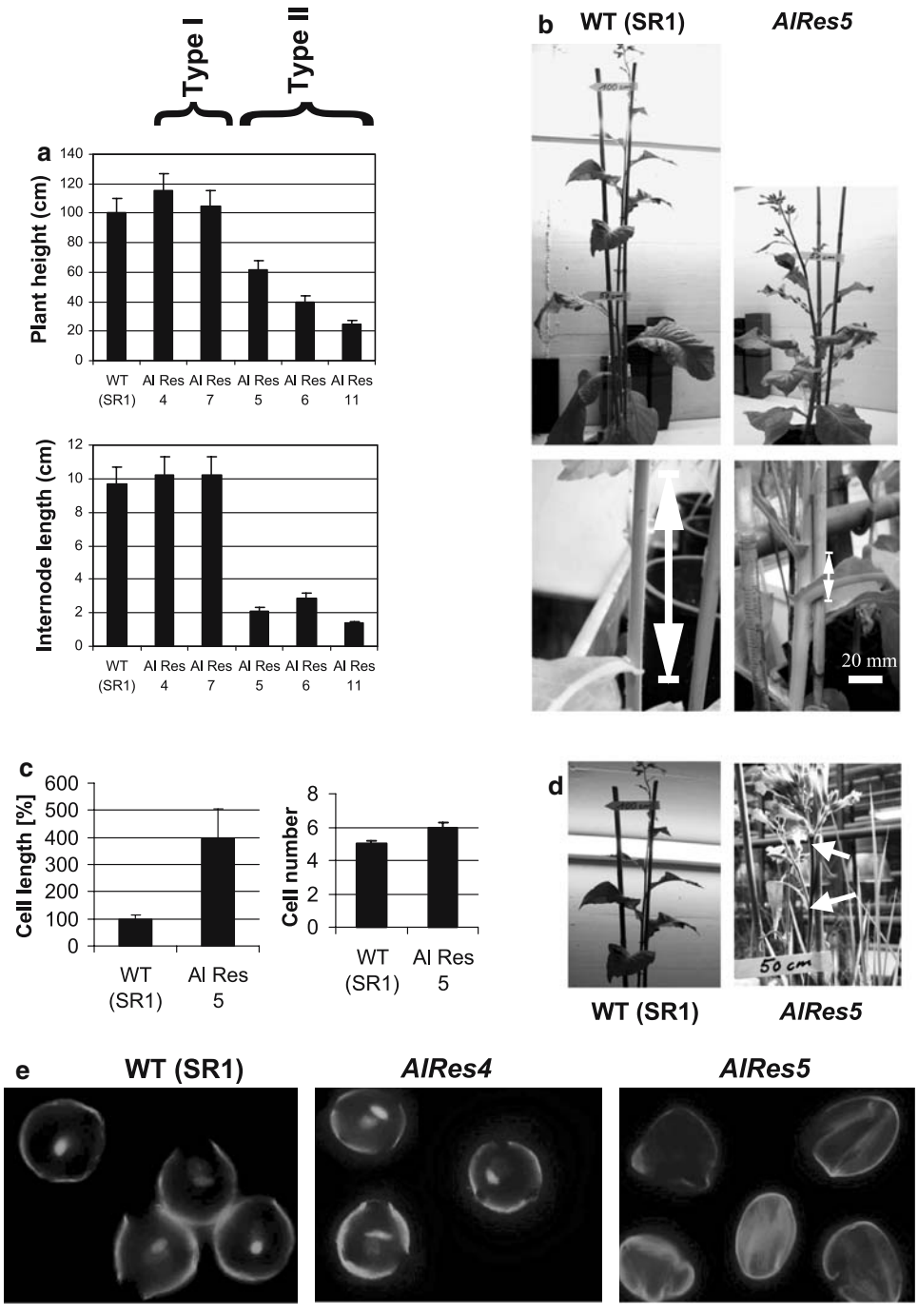

Fig. 2 **a–e** Altered development of *AlRes* mutants. **a** Final plant height and internode length are reduced in mutants of type II, but not of type I. Mean values and standard errors for 5–25 individuals per line. **b** Representative images for mature plants of wild type (SR1) and the type II mutant *AlRes5* showing the semidwarfism and the reduced internodes (*white arrows*) in the mutant. **c** *AlRes* mutants are characterized by increased hairiness. This is accompanied by increased length of hair cells (assayed at leaf petioles) at mostly unreduced number of cells constituting a hair as shown exemplarily for *AlRes5*. **d** *AlRes* mutants of type II exhibit a large number of nodal flowers (*white arrows*) shown exemplarily for *AlRes5*. **e** *AlRes* mutants of type II, but not of type I, are male sterile accompanied by the production of a nuclear pollen. Representative pollen samples stained with DAPI for nuclei are shown for wild type (SR1), *AlRes 4* (fertile, type I) and *AlRes5* (male sterile, type II)

we determined the dose-response relation of leaf expansion (areal increment as percentage of the original area) to latrunculin B (Fig. 4b). In wild type and *AlRes4*, where leaf expansion in the control was comparable, growth was already drastically blocked by 0.1 nM of latrunculin B and this inhibition reached

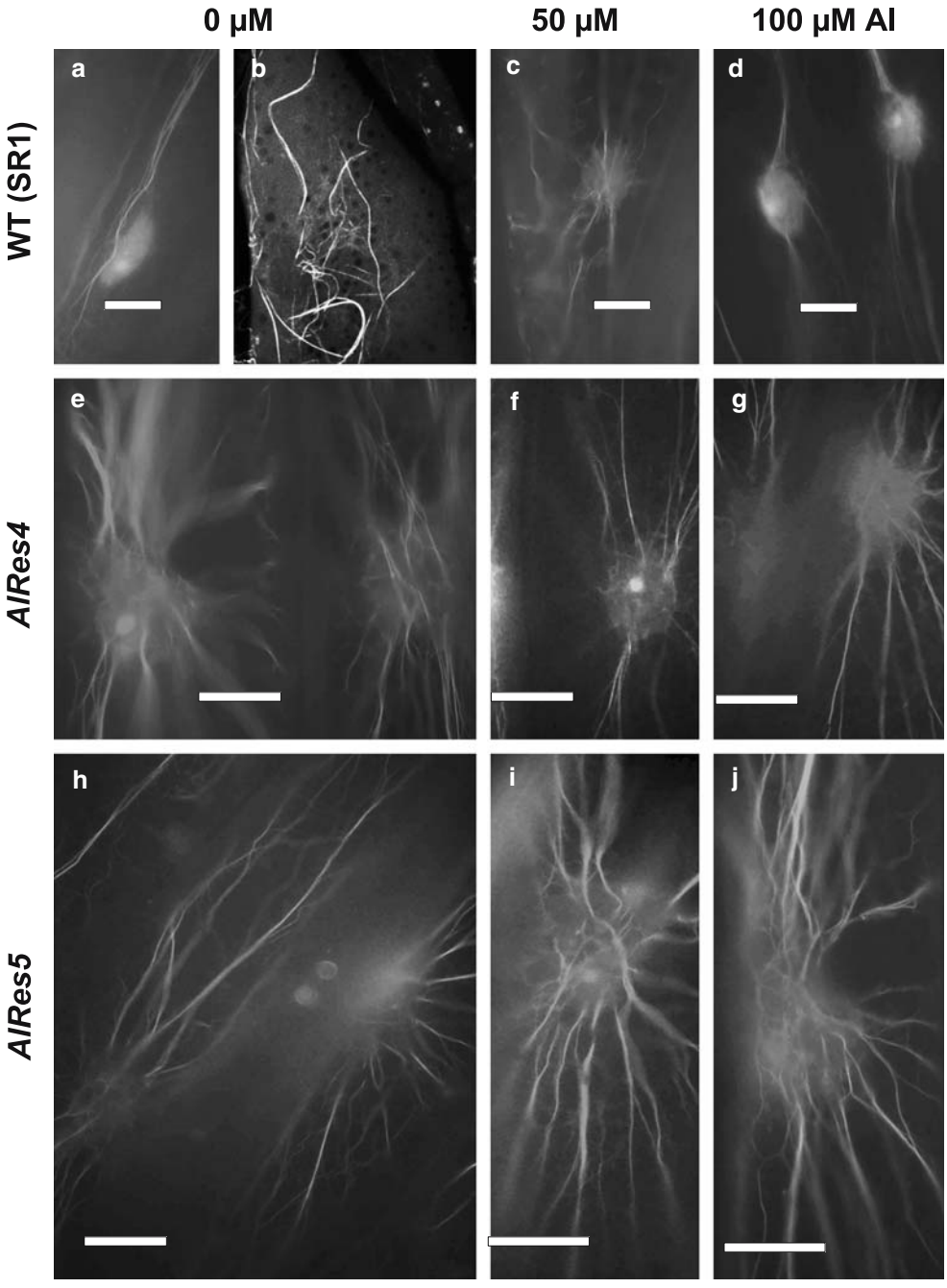

Fig. 3 **a–j** Actin microfilaments are bundled in the *AlRes* mutants. Actin microfilaments in epidermal cells of petioles incubated either in water or in different concentrations of $AlCl_3$ are shown for the wild type (**a–d**), the type I mutant *AlRes4* (**e–g**), and the type II mutant *AlRes5* (**h–j**) in the absence of Al (**a, b, e, h**), and in the presence of 50 µM (**c, f, i**) or 100 µM (**d, g, j**) $AlCl_3$. Note the formation of a perinuclear radial array of actin bundles that occurs in the wild type in response to Al-treatment (compare **a** to **c** and **d**). This array is observed in the mutants already in the absence of Al (**e, h**). *Size bar* 20 µm

saturation at around 50% (wild type) or even 20% (*AlRes4*) of the respective control value. This contrasted with the situation in *AlRes5*, where leaf expansion in untreated controls was reduced as compared to wild type and *AlRes4*. In *AlRes5*, growth persisted mostly even for 10 nM, the highest concentration used in this assay.

The responses of actin microfilaments are accompanied by changes of actin abundance

In the mutants, we observed already in the absence of Al supernumerary actin microfilaments that were often radiating from the nuclear envelope (Fig. 3e–j). This phenotype could be mimicked in the wild type by

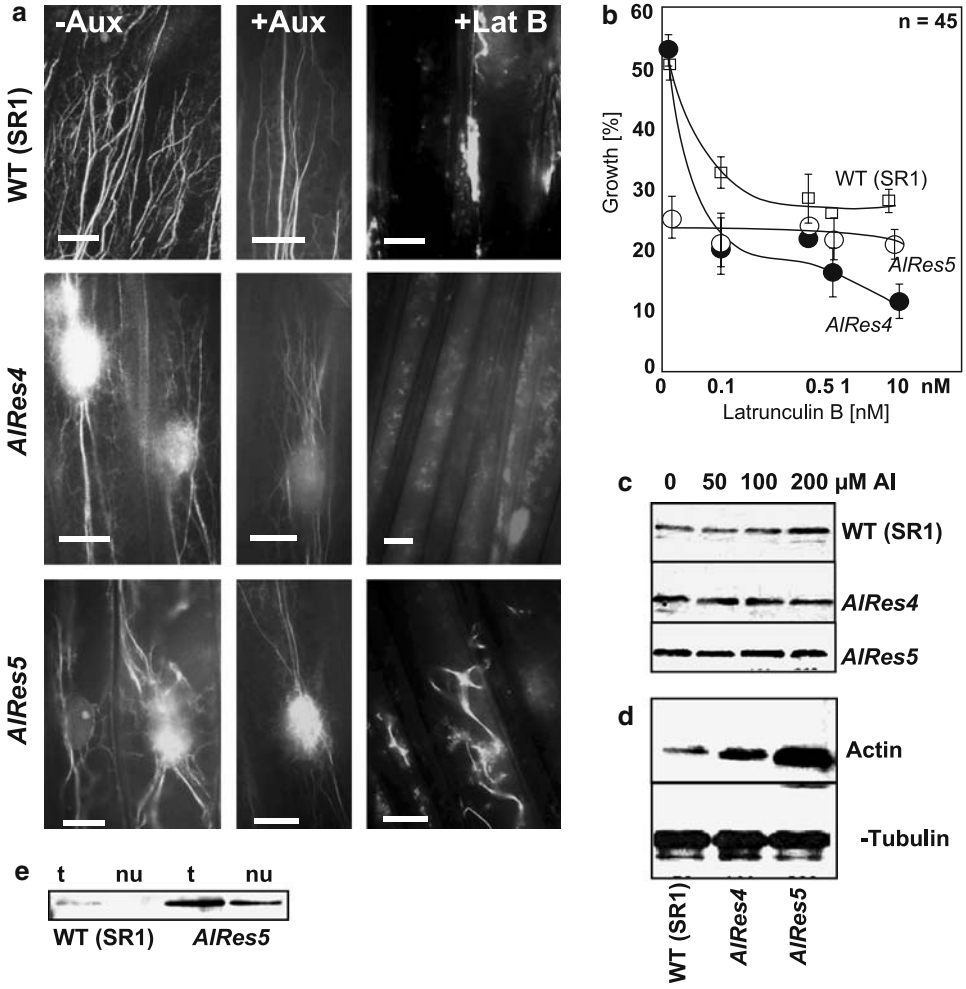

Fig. 4 **a–e** Alterations in the biochemical properties of actin in the *AlRes* mutants. **a** Response of actin microfilaments to latrunculin B, a blocker of actin assembly in the wild type (SR1), the type I mutant *AlRes4*, and the type II mutant *AlRes5*. Note the destruction of the actin cytoskeleton in the wild type and in *AlRes4*, and the partial persistence of actin bundles in *AlRes5*. Latrunculin B (10 nM) was administered for 2 h either in the absence (-auxin) or the presence of 10 µM (+auxin) of indolyl-3-acetic acid. **b** Dose-response relation for leaf expansion over latrunculin B. Wild type (SR1) and the type I mutant *AlRes4* display sensitivity, whereas expansion is reduced, but persistent in the type II mutant *AlRes5*. Data represent mean values and standard errors from at least 20 individuals per experiment. **c** Abundance of actin in total extracts (*upper panel*) and purified nuclei (*lower panel*) from leaves that had been incubated in different concentrations of $AlCl_3$. Note the increase of the actin signal with increasing concentration of Al in the wild type, and the constitutively elevated actin signal in both *AlRes4* and *AlRes5* (10 µg of total protein loaded per lane). Note the strong increase of actin in the mutants over the wild type (20 µg of total protein loaded per lane). **d** For comparison, the *lower panel* shows the tubulin signal obtained for aliquots from the first fraction prior to loading to the Percoll gradient (10 µg of total protein loaded per lane). **e** Abundance of actin in total extracts (t), and nuclear extracts (nu) from wild type versus *AlRes5* (20 µg of total protein loaded per lane)

addition of Al (Fig. 3a–d). We wanted to know whether the supernumerary actin filaments were produced through de novo synthesis of actin or whether they resulted from the dissociation of microfilament bundles. We therefore assayed the abundance of actin in total protein extracts from wild type, *AlRes4* and *AlRes5*, after treatment with different concentrations of Al (Fig. 4c). We observed that, in the wild type, the abundance of actin was increased after treatment with 200 µM $AlCl_3$, whereas it was constitutively elevated in both *AlRes4* and *AlRes5* (most pronounced for *AlRes5*). A direct comparison of actin abundance in relation to α-tubulin that was used as internal standard (Fig. 4d) revealed that even without treatment with Al, actin was significantly more abundant in extracts from *AlRes4*, and drastically more abundant in the extracts from *AlRes5* when compared to extracts from the wild type. To test whether these increases result from the microfilaments that emanate from the nucleus, we purified nuclei from wild type and *AlRes5* and compared equal amounts of total protein with respect to the abundance of actin

(Fig. 4e). We observed that purified nuclei from the wild type contained very little (about 5% as compared to the relative abundance of actin in the total extract) actin, whereas a high proportion (about 38% as compared to the relative abundance of actin in the total extract) of the actin signal observed in total extracts from *AlRes5* could be recovered in purified nuclei. Thus, we observe that the phenotypic response of actin microfilaments (supernumerary microfilaments and actin associated with the nucleus) is accompanied by corresponding changes in the abundance of actin.

Auxin transport is altered in Al-tolerant mutants of type II

All mutants of type II exhibited characteristic changes of leaf-vein patterning, exemplarily shown for *AlRes5* (Fig. 5a). On the macroscopical level, the vasculature appeared to be denser, more reticulate accompanied by a typical buckling of the lamina. On the histological level, the veins were composed of a larger number of vessels (Fig. 5b). This dilatation of vasculature was also detectable in cross section of petioles (Fig. 5c) or internodes (data not shown). Since the pattern of leaf venation is strongly dependent on auxin fluxes, we investigated the uptake of radioactive auxin from an apical donor block in petiole segments from wild type, *AlRes4* and *AlRes5*, which had been either incubated in water or treated with Al (Fig. 5d). In the wild type, the uptake of radioactivity from the apical donor was reduced by Al to about 40% of untreated controls. For *AlRes4*, the uptake was comparable to the wild type, but persistent to Al. For *AlRes5*, the uptake was strongly elevated (by a factor of 5), and, although reduced by $AlCl_3$ treatment, remained strongly elevated as compared to the wild type. A similar pattern was observed for the other mutants of type II as well, although the elevation did not reach the level observed in *AlRes5* (data not shown). Uptake from a donor place to the base of the segment was negligible in all cases (data not shown). To test whether the elevated uptake of radioactivity from an apical donor was accompanied by an increased basipetal transport of auxin within the tissue, we sliced the segments into four sections and measured the radioactivity in each slice separately (Fig. 5e). This approach reveals a clear basipetal gradient of radioactivity with a maximum in the uppermost and a minimum in the lowest slice. In case of *AlRes5*, the radioactivity was elevated in each individual slice by a factor of 2–3 as compared to the corresponding slice of the wild type. This demonstrates that the radioactivity accepted from the donor block is efficiently transported through the tissue. The dilatation of vasculature evident from leaf veins (Fig. 5a, b), and cross sections of petioles (Fig. 5c) is thus accompanied by strongly increased fluxes of auxin through the tissue (Fig. 5d, e).

Discussion

Are the Al-tolerant mutants really tolerant to Al?

We have isolated activation-tagged mutants from a screen, where protoplasts have been challenged with high concentrations of $AlCl_3$. The offspring of the primary transformants was found to be endowed with an elevated tolerance to $AlCl_3$ using cotyledon expansion as parameter (Fig. 1a–c). Despite this correlation there exists the possibility that the mutant phenotype is not caused by a tolerance to $AlCl_3$ for the following reasons: (1) Al might be excluded from the tissue in the mutants and the apparent tolerance of cotyledon growth would then be caused by the exclusion of Al from its target. (2) Al speciates into different forms depending on pH and the concentrations of active Al^{3+} ions are therefore expected to be lower than the nominal concentration of $AlCl_3$.used in the assay.

To address the first issue, we tested root growth in wild type and mutants (Fig. 1d, e), i.e. in the primary target of $AlCl_3$. The comparison of steady-state growth rates showed that the growth rates in the absence of $AlCl_3$ were comparable (Fig. 1d). In contrast, in the mutants the inhibition of growth by $AlCl_3$ was far less pronounced as compared to the wild type. Thus, the Al tolerance of the mutant could be confirmed also on the level of the primary target. We tested whether the inhibition of root growth by $AlCl_3$ might be caused by the acidification of the medium caused by $AlCl_3$ (Table 3). However, acidification in the absence of $AlCl_3$ did not impair root growth, and the inhibition of acidification by buffering did not prevent the $AlCl_3$ effect nor the difference between wild type and mutants. We therefore conclude that the effect of $AlCl_3$ on root growth is a primary effect of Al, and that the mutant phenotype is a true tolerance to Al.

The chemistry of Al in solutions is rather complex. We therefore estimated the active concentration of Al^{3+} based on Kerven et al. (1989) and the GeoChem software. We found that the active concentration of free Al^{3+} under the conditions of our screen amounts to about 80 μM (Table 3), which is in good agreement with estimations from Kollmeier et al. (2000) that report 90 μM of free Al^{3+} for a working solution of 300 μM of $AlCl_3$. For the experiments on actin

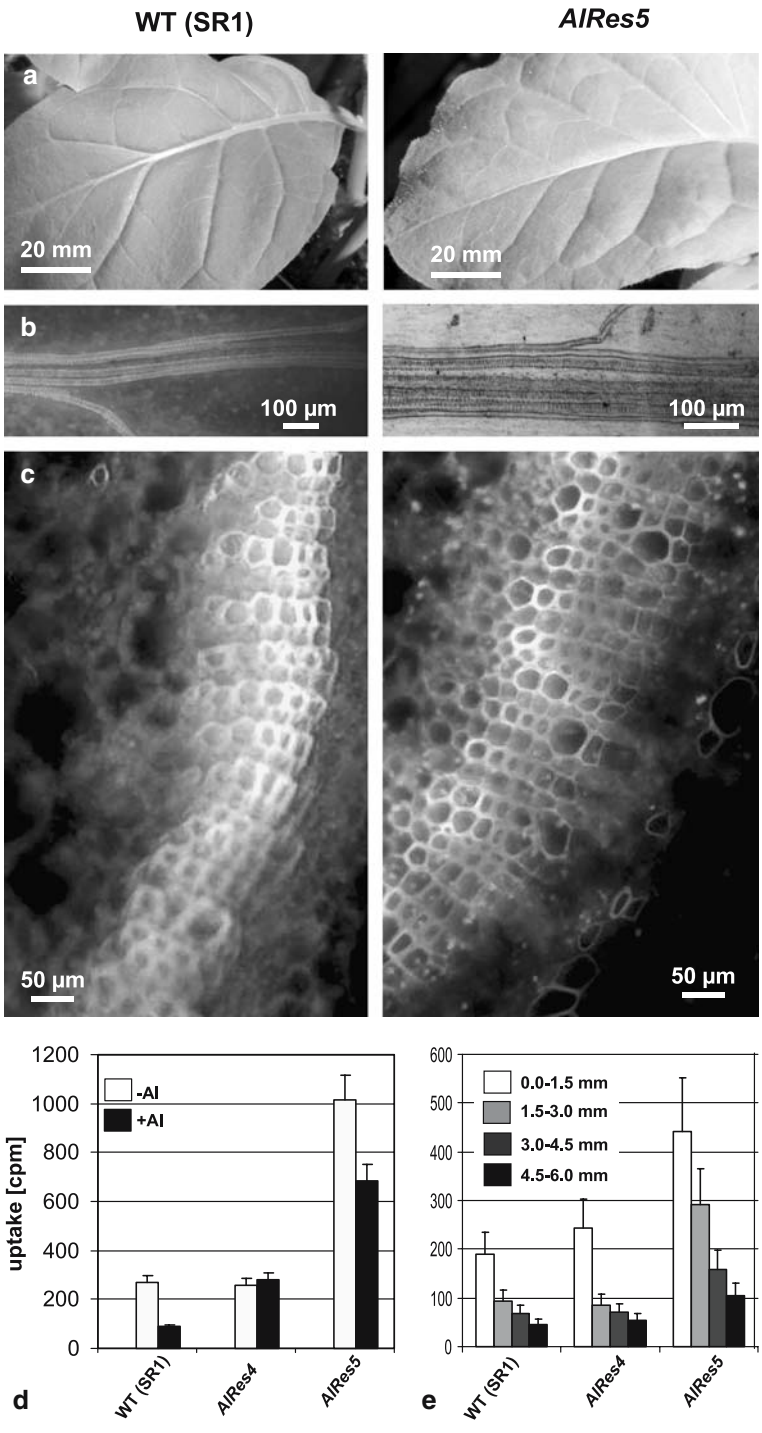

Fig. 5 **a–e** Alterations in vasculature and auxin transport in the *AlRes* mutants. **a** Morphology of adult leaves in wild type (SR1) and *AlRes5*. Note the rough, somewhat buckled leaf surface in the mutant. **b** Close-up of leaf veins in wild type and *AlRes5*; supernumerary vessels are observed in the mutant. **c** Cross section of petioles in wild type and *AlRes5* to demonstrate the dilatated vasculature in the mutant. **d** Polar uptake of radiolabelled auxin into petiole segments of wild type (SR1), the type I mutant *AlRes4*, and the type II mutant *AlRes5* in the absence (*white bars*) and in the presence of 200 µM $AlCl_3$ (*black bars*). **e** Apicobasal distribution of radiolabelled auxin that has been fed to the apical side of petiole segments. Each data set in **d** and **e** was reproduced at least triplicate at different days using five to ten segments from different individuals per experiment

microfilaments and actin levels in leaves that were performed with solutions of $AlCl_3$ in water, a full dissociation into free Al^{3+} is expected.

On the basis of these results, we conclude that the resistance of the mutant protoplasts to our selection protocol was the consequence of elevated tolerance to

Table 3 Changes of pH induced by $AlCl_3$ in the different media used in this study

Type of medium	Concentration of $AlCl_3$ (μM)				Estimated free Al^{3+} in μM for 200 μM of $AlCl_3$
	0	50	100	200	
Water	6.95	5.9	4.7	4.2	200
MS medium	5.5	4.5	4.1	3.8	82
Selective medium	5.0	4.4	4.0	3.8	80

Water was used for the assays on root-growth (Fig. 1d, e), microfilament responses in petioles (Fig. 3). MS medium was used for the assays on leaf expansion (Fig. 1a–c), latrunculin responses (Fig. 4a, b), and auxin-transport in petiole segments (Fig. 5d, e). The selective medium was used for the screen of protoplasts for Al-resistance. The concentration of free Al3+ was estimated using the GeoChem software

Al^{3+}, and that the observed tolerance of mutant roots is a primary manifestation of the selected tolerance to Al^{3+}.

Al-induced responses of actin microfilaments are deregulated in Al-tolerant mutants

The phenotypes of Al-tolerant mutants cluster into two distinct syndromes: in the mutants of type I, the plants were fertile and of normal size, and the transport of auxin was normal, although persistent to Al. In the mutants of type II, the plants were male-sterile and semi-dwarfs, and the transport of auxin was strongly elevated.

The phenotype of type I mutants would be consistent with a mechanism, whereby Al ions are sequestered before they can come into contact with the target cell. Future work on the type I mutants should focus on excretion of organic acids that has been identified in Graminean roots as mechanism to prevent Al ions from reaching the target cells (Piñeros et al. 2005; Sasaki et al. 2004). In the present study as we wanted to get insight into cellular events of the Al response, we focussed on the mutants of type II that displayed obvious changes on the cellular levels, and where morphology and development were altered (stunted growth, male sterility) even when the plant had been never exposed to $AlCl_3$.

In all mutants, irrespective of the syndrome, numerous actin microfilaments emanated from the nuclear envelope and fused to prominent bundles. The formation of supernumerary microfilaments was accompanied by elevated levels of actin protein. Bundling of actin, accompanied by an increase of microfilament rigour has been observed in different plant species as a response to Al (Blancaflor et al. 1998; Grabski and Schindler 1995). As to be expected from the published records, the bundling of actin in Al-tolerant mutants could be phenocopied in the wild type by treatment with Al: Al induced bundling of microfilaments, Al induced numerous microfilaments that emerged from the nuclear envelope, and Al induced the synthesis of actin (Figs. 3, 4). In other words, the responses of the actin cytoskeleton that were induced by Al in the wild type were constitutively activated in the Al-tolerant mutants. This would be consistent with constitutive activation of the Al-induced signal chain that triggers these responses of actin.

The formation of supernumerary microfilaments could be the result of stimulated assembly of F-actin from sequestered pools of G-actin. The responsible signal might be an Al-triggered increase of cytosolic calcium (Rengel and Zhang 2003) that would stimulate the transition from G- to F-actin (Strzelecka-Golaszewska 2001). However, we observe that the abundance of actin protein is stimulated as well, demonstrating that at least a part of the supernumerary microfilaments are produced by actin synthesized de novo.

Despite these general similarities with respect to the altered organization of actin, *AlRes4* as representative of the type I mutants and *AlRes5* as representative of the type II mutants differ with respect to actin dynamics. Actin microfilaments are eliminated by latrunculin B in *AlRes4* and leaf expansion remains sensitive to this drug (Fig. 4). In *AlRes5*, actin microfilaments are rather recalcitrant to latrunculin B and so is leaf expansion that persists up to very high concentrations of latrunculin B. It should be noted that growth was already lower in *AlRes5* as compared to WT and *AlRes4*. Therefore, the persistence of this (low) growth level might just represent the minimal level possible, such that the failure to reduce this residual growth by latrunculin B would not be the manifestation of a true resistance. However, it is possible to inhibit growth to even lower levels in *AlRes4*, when the concentration of latrunculin B is raised. Thus, the reduced, but persistent leaf growth in *AlRes5* is the expression of a true resistance. Since leaf expansion requires cell divisions, it required a relatively long time until the differences

between wild type and mutant became manifest (Fig. 4b). However, latrunculin B is a very potent drug that sequesters G-actin irreversibly (Coué et al. 1987) such that actin microfilaments disappear depending on their innate turnover. Actin microfilaments that are not treadmilling will be more tolerant as compared to actin microfilaments that are endowed with high dynamics of assembly and disassembly. To verify the effect observed in the rather lengthy leaf-disc assay, we tested the response of actin microfilaments directly in short-term experiments (Fig. 4a) and arrived at the same result. Thus, the signal that seems to be activated in *AlRes4* does not alter the dynamics of microfilaments, whereas the signal that is activated in *AlRes5* seems to act as a negative regulator of microfilament turnover.

Interestingly, in both mutants, microfilaments remain responsive to auxin. The bundles are replaced by finer microfilament strands, consistent with the auxin response observed in other systems (Grabski and Schindler 1995; Holweg et al. 2004). Since the two mutants differ with respect to latrunculin B tolerance, the bundling of microfilaments must be caused by a mechanism that is not dependent on actin turnover. This is consistent with recent findings in wheat roots that the bundling of actin is sensitive to myosin inhibitors (Frantzios et al. 2005).

The bundling response of actin to $AlCl_3$ could be interpreted as an adaptive response. If the bundling itself were adaptive, it should not occur in the Al-sensitive wild type, but only in the Al-tolerant mutants. The fact that it is observed in the mutants even in the absence of Al-challenge but is induced in the wild type only upon exposure of the petiole cells to $AlCl_3$ indicates a different scenario: bundling could be merely a downstream event of the primary adaptive response. This is supported by the observation that actin bundling is observed in both type I and type II mutants, whereas type I mutants, in contrast to type II mutants display normal development and morphology (consistent with a possible sequestration of external Al). In other words the two responses must bifurcate. The (putative) activation of Al sequestration in the mutants of class I must be more upstream than the bundling of actin. The actin response (activated in the mutants of class II) can be activated independently, possibly because it is localized at a lower level of the hierarchy.

In fact, there is evidence for a link between actin responses and secretion. For instance, there is a feedback regulation between actin bundling and auxin signalling (for review see Nick 2006). It has been shown that inhibition of exocytosis results in an elevated resistance to $AlCl_3$ in the tobacco cell line BY−2 (Vitorello and Haug 1999). If Al tolerance in the mutant were achieved by such a reduced dynamics of intracellular trafficking, this is expected to result in a reduction of polar auxin transport (for review see Friml 2003), a major target of Al toxicity in roots (Kollmeier et al. 2000; Doncheva et al. 2005). Reduced auxin transport, in turn, will result in bundling of actin microfilaments. Thus, the primary adaptive response would be a down-regulation of vesicle traffic—in the wild type triggered by $AlCl_3$, in the mutants constitutively active as a consequence of the activation tag.

Relationship between Al tolerance and auxin transport in the mutants of type II

The mutants of type II share common traits that indicate auxin transport as a possible target, such as elevated leaf venation, dilatated vasculature in petioles and stems, and (possibly as a consequence) stunted growth. In fact, the uptake of radioactive auxin from a donor as well as the establishment of an apicobasal gradient in the segment was found to be strongly elevated in *AlRes5*. The formation of veins is driven by a redifferentiation of parenchymatic cells in response to polar auxin flux through those cells—since neighbouring cells compete for free auxin there is a lateral inhibition of differentiating vessels on the redifferentiation of the surrounding parenchymatic tissue (for review see Mattson et al. 1999; Sachs 2000). In the context of this canalization model, a generally elevated uptake of auxin (and/or a reduced basipetal efflux of auxin) would lead to broader "channels", i.e. a larger number of cells should initiate vessel differentiation. The morphological phenotype of *AlRes5* (supernumerary veins, dilatated vessels) would be thus consistent with altered ratios between uptake and polar efflux of auxin.

On the cellular level, elevated uptake of auxin is expected to be brought about by changes in the quantity, activity or intracellular localisation of corresponding membrane transporters such as AUX1 (Bennett et al. 1996), whereas reduced polarity of auxin efflux could be caused by mislocalization of the auxin-efflux regulator PIN1 (for review see Friml 2003) or the multidrug resistance protein p-Glycoprotein PGP1 (Geisler et al. 2005). The polar localization of the auxin-efflux regulator PIN1 has to be understood as dynamic equilibrium between endocytosis to endosomes and exocytosis to the plasma membrane (Geldner et al. 2001). This cycling can be manipulated by cytochalasin D, an inhibitor of actin assembly. Conversely, the knockout of the class-XI myosin Mya2 leads to reduced auxin transport and impairs apical dominance in thale cress (Holweg and Nick 2004). Not only PIN1,

but also AUX1 is localized to the cell pole, however, in opposition to PIN1 (Swarup et al. 2001). The bundling of actin observed in the *AlRes* mutants is therefore expected to affect the cycling (and thus localization and activity) of components such as PIN1 or AUX1 which might be the cause for the observed changes in auxin transport characteristics.

The link between actin bundling and auxin transport is also supported from experiments with brefeldin A (BFA). BFA blocks ARF-GEF (a cofactor for small GTPases that are important for vesicle budding) and thus impairs the recycling of PIN1 from the endosomes towards the plasma membrane (Steinmann et al. 1999; Geldner et al. 2003). The same agent induces a dose-dependent bundling of actin in coleoptiles and a concomitant progressive reduction of auxin sensitivity (Waller et al. 2002). We therefore think that the bundling of actin manifest in the *AlRes* mutants will interfere with the dynamic localization of auxin-signalling compounds and thus will affect the regulation of polar auxin transport.

The actual target of Al toxicity is far from being understood, but there is increasing evidence for auxin transport as sensitive target. Acropetal auxin transport in maize roots was strongly stimulated after application of Al to the root cap in contrast to controls, where basipetal transport was prevalent (Hasenstein and Evans 1988). Conversely, radioactive auxin was reported to accumulate in the apical segments of the root after Al treatment to the distal elongation zone (Kollmeier et al. 2000). Recent work showed that the regional patterning within the root tip was shifted by very short exposure to $AlCl_3$ in a characteristic fashion, and this shift could be mimicked by application of the auxin-transport inhibitor NPA (Doncheva et al. 2005). The polarity of auxin transport seems to be linked to the proper allocation of auxin-efflux regulators (such as PIN1) and auxin-influx carriers (such as AUX1) to the opposing poles of the cell, and the findings from maize roots would be consistent with a model, where the polarity of these regulators and/or carriers is perturbed. Interestingly, tobacco cells can be rescued from the toxic effect of Al, when they are pre-treated with BFA (Vitorello and Haug 1999), i.e. under conditions, when PIN1 accumulates in endosomal compartments rather than being recycled to the plasma membrane.

It is therefore conceivable that it is components of auxin efflux that represent a sensitive target for Al. If the dynamic equilibrium of such components were shifted towards endosomal localization, this should cause reduced auxin efflux (accompanied by increased accumulation of auxin in tissues adjacent to the source of auxin) on the one hand, increased tolerance to Al on the other. First attempts to identify sequences flanking the activation tag in type II mutants have led to fragments with homology to cytoskeletal proteins such as tubulins or unconventional myosins. Future work will be dedicated to isolate these target genes and verify their role in Al tolerance by corresponding gain-of-function or loss-of-function experiments. This should allow further insights not only into the cellular target of Al toxicity, but also into the regulation of cell polarity.

Acknowledgments This work was supported by a Volkswagen-Foundation Young Researcher Group Grant (Nachwuchsgruppe) to PN.

References

Ahad A, Wolf J, Nick P (2003) Isolation of tobacco mutants with increased tolerance to low temperature and anticytoskeletal herbicides by activation tagging. Trans Res 12:615–629

Bennet RJ, Breen CM (1991) The aluminum signal: new dimensions to mechanisms of aluminum tolerance. Plant Soil 134:153–166

Bennett MJ, Marchant A, Green HG, May ST, Ward SP, Millner PA, Walker AR, Schulz B, Feldmann KA (1996) Arabidopsis AUX1 gene: a permease-like regulator of root gravitropism. Science 273:948–950

Blancaflor EB, Jones DL, Gilroy S (1998) Alteration in the cytoskeleton accompany aluminum-induced growth inhibition and morphological changes in primary roots of maize. Plant Physiol 118:159–172

Breitling F, Little M (1986) Carboxy-terminal regions on the surface of tubulin and microtubules. Epitope Locations of YOL1/34, DM1A and DM1B. J Mol Biol 189:367–370

Chang C, Kwok SF, Bleecker AB, Myerowitz EM (1993) Arabidopsis ethylene/response gene ETR1: similarity of product to two-component regulators. Science 262:539–544

Chenery EM, Sporne KR (1976). A note on the evolutionary status of aluminum-accumulators among dicotyledons. New Phytol 76:551–554

Coué M, Brenner SL, Spector I, Korn ED (1987) Inhibition of actin polymerization by latrunculin A. FEBS Lett 213:316–318

De la Fuente JM, Ramirez-Rodriguez V, Carbera-Ponce JL, Herrera-Estrella L (1997) Aluminum tolerance in transgenic plants by alteration of citrate synthesis. Science 276:1566–1568

Delhaize E, Ryan PR (1995) Aluminum toxicity and tolerance in plants. Plant Physiol 107:315–321

Delhaize E, Hebb DM, Ryan PR (2001) Expression of a pseudomonas aeruginosa citrate synthase gene in tobacco is not associated with either enhanced citrate accumulation or efflux. Plant Physiol 125:2059–2067

Doncheva S, Amenós M, Poschenrieder C, Barceló J (2005) Root cell patterning: a primary target for aluminium toxicity in maize. J Exp Bot 56: 1213–1220

Foey CD, Chaney RL, White MS (1978) The physiology of metal toxicity in plants. Annu Rev Plant Physiol 29:511–566

Friml J (2003) Auxin transport—shaping the plant. Curr Opin Plant Biol 6:7–12

Frantzios G, Galatis B, Apostolakos P (2005) Aluminium causes variable responses in actin filament cytoskeleton of the root tip cells of *Triticum turgidum*. Protoplasma 225:129–140

Geisler M, Blakeslee JJ, Bouchard R, Lee OR, Vincenzetti V, Bandyopadhyay A, Titapiwatanakun B, Peer WA, Bailly AI, Richards EL, Ejendal KFK, Smith AP, Baroux C, Grossniklaus U, Müller A, Hrycyna CA, Dudler R, Murphy AS, Martinoia E (2005) Cellular efflux of auxin catalyzed by the Arabidopsis MDR/PGP transporter AtPGP1. Plant J 44:179–194

Geldner N, Friml J, Stierhof YD, Jürgens G, Palme K (2001) Auxin transport inhibitors block PIN1 cycling and vesicle trafficking. Nature 413:425–428

Geldner N, Richter S, Vieten A, Marquardt S, Torres-Ruiz RA, Mayer U, Jürgens G (2003) Partial loss of function alleses reveal a role for GNOM in auxin transport-related, postembryonic development of Arabidopsis. Development 131:380–400

Godbolé R, Michalke W, Nick P, Hertel R (2000) Cytoskeletal drugs and gravity-induced lateral auxin transport in rice coleoptiles. Plant Biol 2:176–181

Grabski S, Schindler M (1995) Aluminum induces rigor within the actin network of soybean cells. Plant Physiol 108:897–901

Hasenstein KH, Evans ML (1988) Effects of cations on hormone transport in primary roots of *Zea mays*. Plant Physiol 86:890–894

Hayashi H, Czaja I, Schell J, Walden R (1992) Activation of plant gene by T-DNA tagging: Auxin independent growth in vitro. Science 258:1350–1353

Holweg C, Nick P (2004) Arabidopsis myosin XI mutant is defective in organelle movement and polar auxin transport. Proc Natl Acad Sci USA 101:10488–10493

Holweg C, Süßlin C, Nick P (2004) Capturing in-vivo dynamics of the actin cytoskeleton stimulated by auxin or light. Plant Cell Physiol 45:855–863

Kakimoto T (1996) CKI1, a histidine kinase homologue implicated in cytokinin signal transduction. Science 274:982–985

Kerven GL, Edwards DG, Asher CJ, Hallman PS, Kokot S (1989) Aluminum determination in soil solution. II. Short term calorimetric procedures for the measurement of inorganic monomeric aluminium in the presence of organic acid ligands. Austr J Soil Res 27:91–102

Kochian LV, Hoekenga OA, Piñeros MA (2005) How do crop plants tolerate acid soil? Mechanisms of aluminum tolerance and phosphorus efficiency. Annu Rev Plant Biol 55:459–493

Kollmeier M, Hubert HF, Horst JW (2000) Genotypical differences in aluminum resistance of maize are expressed in the distal part of the transition zone. Is reduced basipetal auxin flow involved in inhibition of root elongation by aluminum? Plant Physiol 122:945–956

Koncz C, Mayerhofer R, Konct-Kalman Z, Nawrath C, Reiss B, Redei GP, Schell J (1990) Isolation of a gene encoding a novel chloroplast protein by T-DNA tagging in *Arabidopsis thaliana*. EMBO J 9:1337–1346

Koncz C, Martini N, Szabados L, Hrouda M, Bachmair A, Schell J (1994) Specialized vectors for gene tagging and expression studies. In: Gelvin SB, Schilperoort RA, Verma DPS (eds) Plant molecular biology manual, vol B2. Kluwer Academic Publishers, Netherlands, pp 1–22

Koop H-U, Steinmüller K, Wagner H, Rössler C, Eibil C, Sacher L (1996) Integration of foreign sequences into the tobacco plastome via polyethylene glycol-mediated protoplast transformation. Planta 199:193–201

MacDonald TL, Martin RB (1988) Aluminum ion in biological systems. Trends Biochem Sci 13:15–19

Mattson J, Sung ZR, Berleth T (1999) Responses of plant vascular systems to auxin transport inhibition. Development 126:2979–2991

Murashige T, Skoog F (1962) A revised medium for rapid growth and bio assays with tobacco tissue cultures. Physiol Plant 15:473–497

Nakazawa M, Ichikawa T, Ishikawa A, Kobayashi H, Tsuhara Y, Kawashima M, Suzuki K, Muto S, Mastui M (2003) Activation tagging, a novel tool to dissect the functions of a gene family. Plant J 34:741–750

Nick P. (2006) Noise yields order: auxin, actin, and polar patterning. Plant Biol 8:360–370

Nick P, Lambert AM, Vantard M (1995) A microtubules-associated protein in maize is induced during phytochrome-dependent cell elongation. Plant J 8:835–844

Nick P, Heuing A, Ehmann B (2000) Plant chaperonins: a role in microtubule-dependent wall formation. Protoplasma 211:234–244

Popov N, Schmitt S, Matthices H (1975) Eine störungsfreie Mikromethode zur Bestimmung des Proteingehalts in Gewebshomogenaten. Acta Biol Ger 31:1441–1446

Piñeros MA, Shaff JE; Manslank HS, Alves VM, Kochian LV (2005) Aluminum resistance in maize cannot solely explained by root organic acid exudation. A comparative physiological study. Plant Physiol 137:231–241

Rengel Z, Zhang W-H (2003) Role of dynamics of intracellular calcium in aluminium-toxicity syndrome. New Phytol 159:295–314

Ryan PR, Delhaize E, Randall PJ (1995) Malate efflux from root apices and tolerance to Al are highly correlated in wheat. Austr J Plant Physiol 22:531–536

Sachs T (2000) Integrating cellular and organismic aspects of vascular differentiation. Plant Cell Physiol 41:649–656

Sasaki T, Yamamoto Y, Ezaki B, Katsuhara M, Ahn SJ, Ryan PR, Delhaize E, Matsumoto H (2004) A wheat gene encoding an aluminum activated malate transporter. Plant J 37:645–653

Schmidt R, Bohm K, Vater W, Unger E (1991) Aluminum-induced osteomalacia and encelopathy: an aberration of the tubulin assembly into microtubules by Al^{3+}. Prog Histochem Cytochem 23:355–364

Schwarzerová K, Zelenková S, Nick P, Opartrný Z (2002) Aluminum induced rapid changes in the microtubular cytoskeleton of tobacco cell lines. Plant Cell Physiol 43:207–216

Sivaguru M, Matsumoto H, Horst WJ (2000) Control of the response to aluminium stress. In: Nick P (ed) Plant microtubules—potential for biotechnology, Springer, Berlin Heidelberg New York , pp 103–120

Sivaguru M, Ezaki B, He Zh-H, Tong H, Osawa H, Baluška F, Volkmann D, Matsumoto H (2003a) Aluminum-induced gene expression and protein localization of a cell wall-associated receptor kinase in Arabidopsis. Plant Physiol 132:2256–2266

Sivaguru M, Pike S, Gassmann W, Baskin TI (2003b) Aluminum rapidly depolymerizes cortical microtubules and depolarizes the plasma membrane: evidence that these responses are mediated by a glutamate receptor. Plant Cell Physiol 44:667–675

Steinmann T, Geldner N, Grebe M, Mangold S, Jackson CL, Paris S, Galweiler L, Palme K, Jurgens G (1999) Coordinated polar localization of auxin efflux carrier PIN1 by GNOM ARF GEF. Science 286:316–318

Strzelecka-Golaszewska H (2001) Divalent cations, nucleotides, and actin structure. Res Probl Cell Differ 32:23–41

Swarup R, Friml J, Marchant A, Ljung K, Sandberg G, Palme K, Bennett M (2001) Localization of the auxin permease AUX1 suggests two functionally distinct hormone transport pathways operate in the Arabidopsis root apex. Genes Dev 15:2648–2653

Tani H, Chen X, Nurmberg P, Grant JJ, SantaMaria M, Chini A, Gilroy E, Birch PRJ, Loake GJ (2004) Activation tagging in

plants: a tool for gene discovery. Funct Integr Genomics 0:1–9

Vitorello VA, Haug A (1999) Capacity for aluminium uptake depends on brefeldin A-sensitive membrane traffic in tobacco (*Nicotiana tabacum* L. cv. BY-2) cells. Plant Cell Rep 18:733–736

Wagatsuma T, Kaneko M, Hayasaka Y (1995) Destruction process of plant root cells by aluminium. Soil Sci Plant Nutr 33:161–175

Waller F, Nick P (1997) Response of actin microfilaments during phytochrome-controlled growth of maize seedlings. Protoplasma 200:154–162

Waller F, Riemann M, Nick P (2002) A role for actin-driven secretion in auxin-induced growth. Protoplasma 219:72–81

Watt DA (2003) Aluminium-responsive genes in sugarcane: identification and analysis of expression under oxidative stress. J Exp Bot 54:1163–1174

Weigel D, Ahn JH, Blazquez MA et al (2000) Activation tagging in Arabidopsis. Plant Physiol 122:1003–1013

Xia Y, Suzuki H, Borevitz J, Blount J, Guo Z, Patel K, Dixon RA, Lamb C (2004) An extracellular aspartic protease functions in Arabidopsis disease resistance signaling. EMBO J 23:980–988

Yang JL, Zheng SJ, He YF, Matsumoto H (2005) Aluminum resistance requires resistance to acid stress: a case study with spinach that exudes oxlate rapidly when exposed to Al stress. J Exp Bot 56:1197–1203

Zubko E, Adams CJ, Machaelkova I, Malbeck J, Scollan C, Meyer P (2002) Activation tagging identifies a gene from *Petunia hybrida* responsible for the production of active cytokinins in plants. Plant J 29:797–808